

Silver and Gadolinium Ions Co-substituted Hydroxyapatite Nanoparticles as Bimodal Contrast Agent for Medical Imaging

Madhumathi K¹, Sampath Kumar TS^{1*}, Mohammed Sanjeed T², Sabik Muhammed A², Sahal Nazrudeen² and Sharanya D³

¹Medical Materials Laboratory, Department of Metallurgical and Materials Engineering, Indian Institute of Technology Madras, Chennai 600042, India

²Department of Biomedical Engineering, SMK Fomra Institute of Technology, Kelambakkam, Chennai 603103, India

³Department of Biomedical Engineering, Sri Ramakrishna Engineering College, Vattamalaipalayam, N.G.G.O colony post, Coimbatore 641022, India

Abstract

Developing multimodal contrast agents is an upcoming area and hydroxyapatite nanoparticles substituted with various elements like gadolinium, europium etc., seems to be a promising contrast agent, especially for multimodal imaging of bone-tissue interface. A bimodal contrast agent using silver (Ag⁺) and gadolinium (Gd³⁺) ions co-substituted hydroxyapatite nanoparticles has been developed for X-ray and magnetic resonance imaging. Ag⁺ and Gd³⁺ ions were co-substituted into hydroxyapatite at various atomic percentages (Ag:Gd=0.25:0.25, 0.25:0.5, 0.25:0.75) using microwave accelerated wet chemical synthesis. Pure as well as Ag⁺ and Gd³⁺ ions substituted hydroxyapatite samples were also synthesized for comparison. All samples were characterized by X-ray diffraction, Fourier transform infrared spectroscopy, transmission electron microscopy etc., and found to be monophasic, nanocrystalline with the substituted ions. These co-substituted hydroxyapatite samples were then tested in different diagnostic modalities such as X-ray, computed tomography imaging and magnetic resonance imaging. Appreciable variation in contrast was observed with different amount of substitutions. All the Ag⁺ and Gd³⁺ ions co-substituted hydroxyapatite nanoparticles showed higher contrast in all imaging modalities compared to those substituted with either Ag⁺ or Gd³⁺ ions only. Hydroxyapatite sample co-substituted with 0.25Ag and 0.75Gd at % substitution showed the best bimodal CT-MRI contrast.

Keywords: Hydroxyapatite; Bimodal imaging; CT-MRI contrast; Silver-gadolinium substitution; Nanoparticles

Introduction

Currently, various non-invasive imaging modalities such as computed X-ray tomography (CT), magnetic resonance imaging (MRI), ultrasound imaging (USI), positron emission tomography (PET) and single photon emission spectroscopy (SPECT) are used in the diagnosis of various diseases [1,2]. Each imaging modality has its own applications, merits and demerits. Since, a single imaging technique does not give a complete perspective on all aspects of a disease/disorder, it is common in clinical practice to rely on two or more techniques to arrive at an accurate and reliable diagnosis. For example, combinations of CT/MRI, PET/SPECT etc., are used for radiation treatment planning and cancer diagnosis respectively [1,2]. Hence, multimodal imaging is a rapidly advancing field given its clinical importance with improved patient safety and lowered cost. Multimodal imaging implicates combining several imaging techniques by developing multifunctional contrast agents. Until now, only separate contrast agents are used for each imaging mode like iodine or barium compounds as radio contrast agents for X-ray/CT imaging, paramagnetic Gd³⁺ compounds and super paramagnetic iron oxide (SPIO) nanoparticles for MR imaging [3]. Studies are being carried out to combine different modes of imaging by developing a single contrast agent based on polymers, liposomes and inorganic nanoparticles like hydroxyapatite (HA) [3,4]. Some of the ideal properties required for a contrast agent include colloidal stability independent of pH and temperature variations, high selectivity and sensitivity, sufficient blood circulation time and easy renal clearance [5,6]. Multimodal contrast agents based on inorganic nanoparticles have attracted considerable attention due to their small tunable size and attractive physical and chemical properties including bio-functionalization, prolonged circulating half-life, passive accumulation at tumor site through enhanced permeation and retention (EPR) effect [5]. The nanoparticulate contrast agents have been reported to provide enhanced signal sensitivity and impart information at the cellular levels [7].

Bioceramics like hydroxyapatite (HA, mineral component of bone)

which has been extensively studied as a bone substitute or drug delivery carrier has also shown potential as a contrast agent when substituted with various ions like Gd³⁺, Eu³⁺, Tb³⁺ etc., for MRI and fluorescent imaging [8-10]. HA nanoparticles are non-toxic and provide flexibility in terms of ion substitutions in the crystal structure. They also contain multiple functional groups enabling targeted imaging and provide the diagnostic value by serving as drug carriers as well [11,12]. These properties make nano HA as an attractive multimodal contrast agent. Among all the imaging techniques, CT and MRI are widely used clinically and thus developing a single CT-MRI contrast agent may enhance the imaging capabilities especially at the bone-tissue interface.

MRI is a non-ionizing imaging method that offers a high soft tissue contrast and provides high spatial resolution. This technique is based on measuring water proton relaxation states under a magnetic field [5,13]. Gadolinium (III) or Gd³⁺ ion is a commonly used positive contrast for MRI by enhancing the T1 relaxation in T1 weighed images. Gd³⁺ ion has been incorporated into silica, carbon nanotubes etc., to provide brighter MR signal [14,15]. CT is the most powerful imaging technique employing X-ray ionization and found to be very ideal for hard tissue imaging [5]. Iodinated nanoparticles, gold nanoparticles, iron oxide nanoparticles etc., are popular nanoparticulate contrast agents studied for CT/X-ray imaging [5]. In our study, we have co-

*Corresponding author: Sampath Kumar TS, Medical Materials Laboratory, Department of Metallurgical and Materials Engineering, Indian Institute of Technology Madras, Chennai 600042, India, Tel: +91 4422574772; E-mail: tssk@iitm.ac.in

Received October 08, 2014; Accepted October 24, 2014; Published October 31, 2014

Citation: Madhumathi K, Kumar TS, Sanjeed MT, Muhammed SA, Nazrudeen S, et al. (2014) Silver and Gadolinium Ions Co-substituted Hydroxyapatite Nanoparticles as Bimodal Contrast Agent for Medical Imaging. *Bioceram Dev Appl* 4: 079. doi: 10.4172/2090-5025.1000079

Copyright: © 2014 Madhumathi K, et al. This is an open-access article distributed under the terms of the Creative Commons Attribution License, which permits unrestricted use, distribution, and reproduction in any medium, provided the original author and source are credited.

substituted Ag^+ and Gd^{3+} ions into HA crystal structure to develop a bimodal CT-MRI contrast agent. Although silver in colloidal form was used as early as 1905 as a radiographic contrast agent, its usage was discontinued owing to its high toxicity [16]. However, it has been shown earlier that, the toxicity issues associated with silver can be resolved, by silver substitution in low amounts (0.25 at %) into HA crystal structure, with *in vitro* biocompatibility studies [17]. In the present study, Ag^+ and Gd^{3+} ions co-substituted HA nanoparticles were synthesized and the contrast enhancement provided by the substituted HA nanoparticles were evaluated through X-ray, CT imaging and MR imaging. For comparison, pure HA nanoparticles without any substitution and with only either 0.25% Ag^+ ion substitution or with 0.25-1% Gd^{3+} ion substitution were also synthesized and evaluated for their contrast properties.

Materials and Methods

Pure and ion substituted HAs were prepared as reported earlier [17,18]. Calcium nitrate, diammonium hydrogen phosphate, silver nitrate and gadolinium oxide (Analytical grade, Merck limited, Mumbai) were used as the precursors. The amount of precursors was calculated to synthesize ion substituted HAs using a rapid microwave accelerated wet chemical synthesis method with Ag^+ ion concentration fixed at 0.25 at % and varying the Gd^{3+} ion concentration to a maximum of 0.75 at %. The Ca/ P, (Ca⁺ Ag)/ P, (Ca⁺ Gd)/ P and (Ca⁺ Ag⁺ Gd)/ P ratios were maintained at 1.67. The resultant ion substituted samples were coded as listed in Table 1. The synthesized samples were characterized for structural and phase purity using X-ray powder diffraction (XRD, D8 Discover, Bruker, Germany) with CuK α radiation (1.54 Å). The diffraction patterns were recorded at a scanning rate of 1 step/ s with step size of 0.1 °/ step. The functional groups of the synthesized powders were assayed using a Fourier transform infrared spectroscopy (Spectrum Two FT-IR spectrometer, Perkin-Elmer, USA) in the attenuated internal reflection (ATR) mode. The spectra were collected in the spectral range of 400-510 cm^{-1} . The transmission electron microscopy (TEM) analysis was carried out by dispersing the samples in acetone and irradiated with ultrasonic for 12-15 min in an ultrasonic bath (Citizen, India). The dispersions were then dropped on carbon-coated copper grids, dried, and examined for morphology with a TEM (Philips CM20 TEM, Netherlands) operated at 120 kV. The image contrast properties of the samples were then studied using radiography (X-ray), CT and MRI. The powder samples were weighed and compressed into pellets of one cm diameter and of equal weight. The radiographs were taken in high frequency X-ray generator (Siemens Multiphos 15, USA) along with aluminium standards of 1-5 mm thickness to quantify the contrast values. For CT scan, the pellets were placed inside a phantom model and imaged using a 6-slice spiral CT (Philips Ingenuity Core128, USA) in a coronal section. For MRI imaging, 50 mg of each powder was dispersed in 200 ml of distilled water. The dispersed samples were placed within a phantom model and imaged using a MRI (GE Healthcare, USA) of 1.5 tesla. Digital imaging and communications in medicine (DICOM) software [NEMA, USA] was used to view the CT and MRI images.

Results

Typical XRD patterns of the co-substituted HA samples are shown in Figure 1 along with pure HA pattern for comparison. The XRD pattern of the substituted HAs exhibits peaks similar to pure HA (JCPDS 09-432). The cell parameters and cell volume were calculated using 'Unitcell' software and the values are listed in Table 1. The cell parameters were found to increase with Ag^+ substitution in AGHA sample

and decrease with Gd^{3+} substitution for the GDHA samples. The co-substituted HA samples showed larger cell parameters relative to other samples. Scherrer's formula [$t=0.9\lambda/B\cos\theta$] was used to calculate the crystallite size (t) using the wavelength (λ) of CuK α radiation and full width at half-maximum value (B in radians) of the diffraction peak at 26° (2 θ). The crystallite size obtained from XRD results also showed a larger range of 43-51 nm for the co-substituted samples compared to substituted and pure HA samples which exhibited a size range of about 40-45 nm. The functional groups present in various ions substituted HA were identified from FT-IR spectra. Typical FT-IR spectra of pure and co-substituted HA are shown in Figure 2. All the vibration bands correspond to that of characteristic bands of HA. The substituted HA sample in addition show carbonate bands [19]. The TEM images Figure 3 indicate that the nanoparticles have a rod/acicular morphology. Co-substituted HA samples namely, 25AG50GDHA and 25AG-75GDHA showed a slightly larger size than pure and ion substituted HA nanoparticles. The particle sizes calculated from TEM micrographs using Image J image analysis software are listed in Table 1.

The X-ray radiographical images of the pure and substituted HA samples are shown in Figure 4. The ion substituted samples exhibited higher contrast than pure HA. Figure 4b shows the grayscale value graph in which the contrast has been quantified with respect to the thickness of aluminium standards (1-5 mm). The gadolinium substituted samples showed an increase in contrast with increased amount of substitution. Similar trend was also observed in co-substituted HA samples. It can be seen that 25AG75GDHA shows highest contrast among all the samples with a grayscale value of 2.34 (Al thickness).

The CT scan radiograph with various ion substituted HA samples are shown in Figure 5. The contrast values are indicated in Hounsfield Units (HU). As with X-ray imaging, the co-substituted HA samples exhibited better contrast compared to both pure and substituted HA samples. MRI scan was done on the pure and substituted HA samples and the MR image is shown in Figure 6. All ion substituted samples showed a higher MRI contrast in the T1 relaxation mode compared to pure HA.

Discussion

The main aim of the study was to develop a bimodal contrast agent for CT-MR imaging by substituting Ag^+ and Gd^{3+} cations in the crystal structure of HA nanoparticles. One of the main criteria in deciding the percentage of Ag^+ and Gd^{3+} ion substitutions in HA was biocompatibility. Previous reports have shown that the Ag^+ and Gd^{3+} ion substitutions in HA have been found to be biocompatible at up to 0.25 at % [17] and 4.4 at % [3] respectively. Hence, the silver concentration was fixed at 0.25 at % and the maximum combined substitution ($\text{Ag}^+ + \text{Gd}^{3+}$) in HA were restricted to ≤ 1 at % to have a biocompatible contrast agent.

Ion substituted HAs were characterized using XRD to confirm the phase purity and to evaluate the variations in lattice parameters. Both Ag^+ and Gd^{3+} cations can be substituted in place of Ca^{2+} ions. The absence of any other peaks in XRD confirmed that the samples are phase pure and are not affected by ion substitutions. AGHA sample showed larger lattice parameters and cell volume due to the substitution of larger size Ag^+ (ionic radii) ions for Ca^{2+} ions. In case of GDHA, a reduction in cell parameters was observed due to the substitution of smaller size Gd^{3+} ions Table 1. A reduction in 'c' axis was observed with all GDHA samples. These results are agreeing with the reported values [17,18]. The co-substituted HA samples showed larger cell parameters compared to pure HA with an increase in 'a' axis. Similarly, both XRD and TEM results. Table 1 show that the AGHA and co-substituted HA

Sample Code	Amount of ion substitution (In atomic %)	Cell parameters (Å)		Cell volume (Å) ³	Crystallite size(nm)	
		A	C		XRD	TEM (lxb)
HA	-	9.37	6.8	507	42	38x5
25AGHA	0.25 % Ag ⁺	9.39	6.9	512	45	42x5
25GDHA	0.25 % Gd ³⁺	9.29	6.34	502	41	34x5
50GDHA	0.50 % Gd ³⁺	9.29	6.3	502	42	39x5
75GDHA	0.75 % Gd ³⁺	9.29	6.3	503	41	39x4
100GDHA	1% Gd ³⁺	9.29	6.3	518	40	38x4
25AG25GDHA	0.25 % Ag ⁺ and 0.25 % Gd ³⁺	9.29	6.8	743	43	39x4
25AG50GDHA	0.25 % Ag ⁺ and 0.50% Gd ³⁺	10.02	6.8	749	50	52x6
25AG75GDHA	0.25 % Ag ⁺ and 0.75 % Gd ³⁺	10.17	6.8	757	51	58x6

Table 1: List of cell parameters, cell volume and crystallite size obtained from XRD and TEM results.

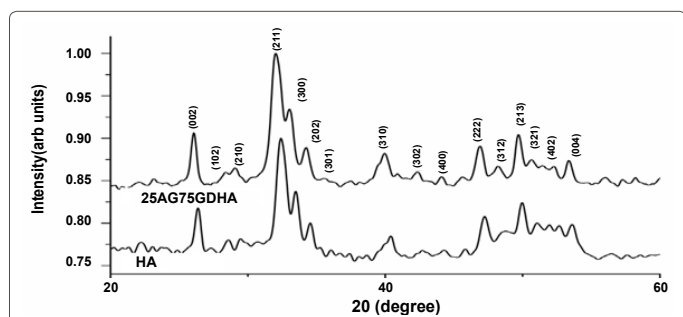


Figure 1: Typical XRD pattern of HA and ion substituted HA nanoparticles

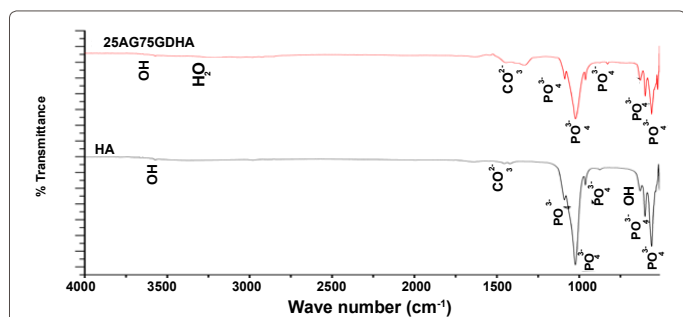


Figure 2: Typical FT-IR spectra of HA and ion substituted HA nanoparticles

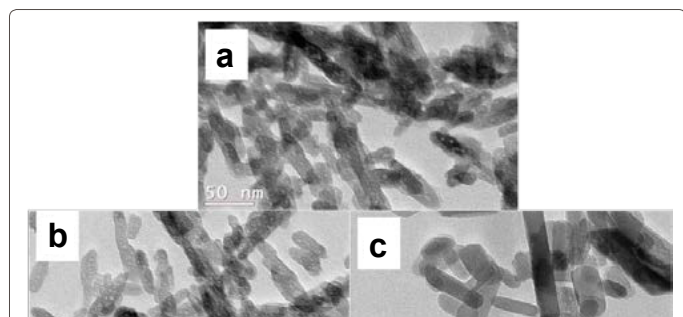


Figure 3: Typical TEM image of a) 25AGHA b) 100GDHA and c) 25AG75GDHA nanoparticles

nanoparticles are of larger size while GDHAs are generally smaller than the HA nanoparticles. Thus, the particle size obtained from TEM mostly correlates with the crystallite size obtained from XRD. The purity of ion substituted HA samples was further confirmed by FT-IR spectra. The ion substituted samples, however, seem to be susceptible to CO₂

adsorption than pure HA [20].

The X-ray radiographs show that both Ag⁺ and Gd³⁺ ions contribute to the radiocontrast of all substituted HA samples. In case of co-substituted HA samples, the radiopacity is primarily due to Gd³⁺ ion substitution with substantial contribution from Ag⁺ ions as also indicated by the grayscale values. A detailed analysis of CT scan results also show that co-substituted HA samples show higher contrast compared to other samples. The pure HA had a value of 1011 HU,

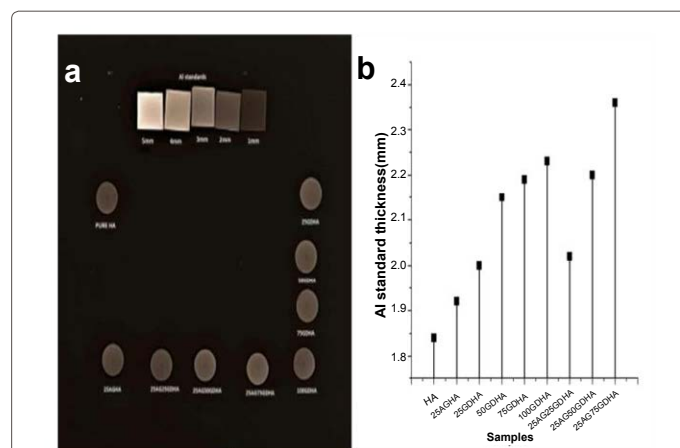


Figure 4: X-ray image (a) and corresponding grayscale value graph (b) of pelletised samples. The aluminium standards are shown in figure 3a (top).

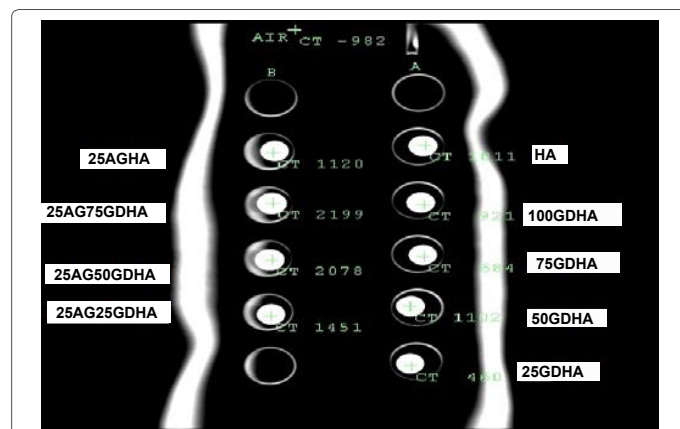


Figure 5: CT scan image of pelletized ion substituted samples with radio contrast in Hounsfield units (HU).

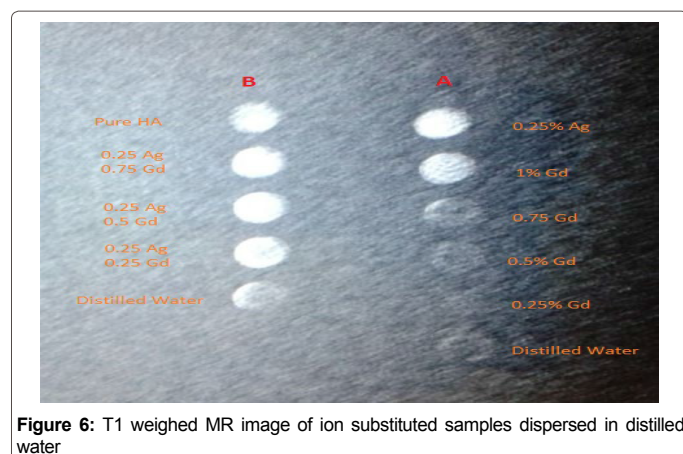


Figure 6: T1 weighed MR image of ion substituted samples dispersed in distilled water

which increased to 1120 HU with the substitution of silver. Similarly, with gadolinium substitution, the 50GDHA sample exhibited a maximum value of 1112 HU. Among co-substituted HA samples, 25AG75GDHA showed the highest contrast of 2199 HU. Although it is well known that silver provides radiographic contrast, the present study shows that gadolinium substitution further enhances the contrast in CT scan. The MR imaging data shows that the co-substituted 25AG50GDHA and 25AG75GDHA pellets exhibit superior contrast due to Gd^{3+} substitution. The X-ray, CT and MRI results clearly reveal that Ag^+ and Gd^{3+} co-substituted HA samples exhibit good bimodal contrast compared to pure and substituted HA samples.

Conclusions

Bimodal contrast agent based on Ag^+ and Gd^{3+} co-substituted HA was prepared using a rapid microwave accelerated wet chemical synthesis with the total substitution not exceeding one at %. The samples showed consistently high contrast in X-ray, CT and MR imaging modalities even at low concentrations. The 25AG75GDHA sample showed the best bimodal contrast. Thus Ag^+/Gd^{3+} ion substituted HAs appear to be a promising contrast medium for combined X-ray/CT-MRI imaging.

Acknowledgements

We are thankful to the Institute Hospital, IIT Madras and Department of Radiology, Chettinad Super Speciality Hospital, Chettinad Health City, Chennai, India for the timely help with X-ray, CT and MR imaging.

References

1. Metcalfe P, Liney GP, Holloway L, Walker A, Barton M, et al. (2013) The potential for an enhanced role for MRI in radiation-therapy treatment planning. *Technol Cancer Res T* 12: 429-446.
2. Van Dort ME, Rehemtulla A, Ross BD (2008) PET and SPECT Imaging of tumor biology: New approaches towards oncology drug discovery and development. *Curr Comput-Aid Drug* 4: 46-53.

3. Anusha A, Deepthy M, Shantikumar N, Manzoor K (2010) A molecular receptor targeted, hydroxyapatite nanocrystal based multi-modal contrast agent. *Biomaterials* 31: 2606-2616.
4. Sonali S, Deepthy M, Adersh A, Shantikumar N, Manzoor K (2010) Folate receptor targeted, rare-earth oxide nanocrystals for bi-modal fluorescence and magnetic imaging of cancer cells. *Biomaterials* 31: 714-729.
5. Trequesser QL, Seznec H, Delville MH (2013) Functionalized nanomaterials: their use as contrast agents in bioimaging: mono- and multimodal approaches. *Nanotechnol Rev* 2: 125-169.
6. Hahn MA, Singh AK, Sharma P, Brown SC, Moudgil BM (2011) Nanoparticles as contrast agents for in-vivo bioimaging: current status and future perspectives. *Anal Bioanal Chem* 399: 3-27.
7. Cheon J, Lee JH (2008) Synergistically integrated nanoparticles as multimodal probes for nanobiotechnology. *Acc Chem Res* 41: 1630-1640.
8. Mondejar SP, Kovtun A, Epple M (2007) Lanthanide-doped calcium phosphate nanoparticles with high internal crystallinity and with a shell of DNA as fluorescent probes in cell experiments. *J Mater Chem* 17: 4153-4159.
9. Altinoglu EI, Russin TJ, Kaiser JM, Barth BM, Eklund PC, et al. (2008) Nearinfrared emitting fluorophore-doped calcium phosphate nanoparticles for in vivo imaging of human breast cancer. *ACS Nano* 2: 2075-2084.
10. Liun Z, Wang Q, Yao S, Yang L, Yu S, et al. (2014) Synthesis and characterization of Tb^{3+}/Gd^{3+} dual-doped multifunctional hydroxyapatite nanoparticles. *Ceram Int* 40: 2613-2617.
11. Anusha A, Genekehal SG, Vijay HS, Arun B, Reshmi P, et al. (2013) Multifunctional calcium phosphate nano-contrast agent for combined nuclear, magnetic and near-infrared in vivo imaging. *Biomaterials* 34: 7143-7157.
12. Chen F, Huang P, Zhu YZ, Wu J, Zhang CL, et al. (2011) The photoluminescence, drug delivery and imaging properties of multifunctional Eu^{3+}/Gd^{3+} dual-doped hydroxyapatite nanorods. *Biomaterials* 32: 9031-9039.
13. Bridot JL, Faure AC, Laurent S, Riviere C, Billotey C, et al. (2007) Hybrid Gadolinium Oxide Nanoparticles: Multimodal Contrast Agents for in Vivo Imaging. *J Am Chem Soc* 129: 5076-5084.
14. Na HB, Hyeon T (2009) Nanostructured T1 MRI contrast agents. *J Mater Chem* 19: 6267-6273.
15. Ribot EJ, Miraux S, Konsman JP, Bouchaud V, Pourtau L, et al. (2011) In vivo MR tracking of therapeutic microglia to a human glioma model. *NMR Biomed* 24: 1361-1368.
16. Yu SB, Alan DW (1999) Metal-Based X-ray Contrast Media. *Chem Rev* 99: 2353-2377.
17. Rameshbabu N, Sampath Kumar TS, Prabhakar TG, Sastry VS, Murthy KV, et al. (2007) Antibacterial nanosized silver substituted hydroxyapatite: Synthesis and characterization. *J Biomed Mater Res A* 80: 581-591.
18. Getman EI, Loboda SN, kachenko TV, Yablochkova NV, Chebyshev KA (2010) Isomorphous Substitution of Samarium and Gadolinium for Calcium in Hydroxyapatite Structure. *Russ J Inorg Chem* 55: 333-338.
19. Sivakumar KM, Sampath Kumar TS, Shantha KL, Rao P (1996) Development of hydroxyapatite derived from Indian coral. *Biomaterials* 17: 1709-1714.
20. Siva Rama Krishna D, Siddharthan A, Seshadri SK, Sampath Kumar TS (2007) A novel route for synthesis of nanocrystalline hydroxyapatite from eggshell waste. *J Mater Sci: Mater Med* 18: 1735-1743.